Cureus Journal of Computer Science

Open Access Original Article

# Corrected: Phenylephrine's Heterogeneous Renal Effects in Non-Cardiac Surgery: A Causal Machine Learning Study

**Received** 10/23/2025
**Review began** 10/26/2025
**Review ended** 12/13/2025
**Published** 12/22/2025
**Corrected** 01/02/2026

**© Copyright** 2025
Cui et al. This is an open access article distributed under the terms of the Creative Commons Attribution License CC-BY 4.0., which permits unrestricted use, distribution, and reproduction in any medium, provided the original author and source are credited.

**DOI:**
https://doi.org/10.7759/s44389-025-00018-2

Junqi Cui [1] , Enoch Chi Ngai Lim [2] , Xiaoqin Wu [3] , Chi Eung Danforn Lim [4]

1. School of Health Sciences, University of New South Wales, Kensington, AUS 2. Translational Research Department, Specialist Medical Services Group, Earlwood, AUS 3. Department of Chinese Medicine, Sydney Institute of Traditional Chinese Medicine, Sydney, AUS 4. NICM Health Research Institute, Western Sydney University, Westmead, AUS

**Corresponding author:** Chi Eung Danforn Lim, cmo@smsg.au

## This article has been corrected.

Correction date: January 02, 2026. Cite this correction as Cui J, Lim E, Wu X, et al. (January 02, 2026) Correction: Phenylephrine's Heterogeneous Renal Effects in Non-Cardiac Surgery: A Causal Machine Learning Study. Cureus J Comput Sci 3 : es44389-026-00003-3. doi:https://dx.doi.org/10.7759/s44389-026-00003-3.

The original online version of this article was revised at the request of author.

**Author Name:**

Incorrect: Xiqoqu WU

Correct: Xiaoqin WU

**Affiliation:**

Incorrect: Department of Chinese Medicine, Endeavour College of Natural Health, Sydney, AUS

Correct: Department of Chinese Medicine, Sydney Institute of Traditional Chinese Medicine, Sydney, AUS

## Abstract

### Background

Phenylephrine is widely used to manage intraoperative hypotension during intermediate-to-major non-cardiac surgeries, yet its effects on renal function vary considerably across individuals. Identifying the underlying sources of this heterogeneity is essential for developing precision perioperative strategies.

### Methods

Data from the high-resolution VitalDB dataset was utilised. Individual treatment effect was estimated using augmented inverse probability of treatment weighting, T-Learner, and X-Learner algorithms. Heterogeneity was assessed through subgroup stratification, causal decision trees, and SHapley Additive exPlanations-based interpretation.

### Results

Among 3,017 adult patients, intraoperative phenylephrine use was associated with a modest overall decline in postoperative glomerular filtration rate, accompanied by substantial inter-individual heterogeneity. Across multiple causal machine learning models, clinically meaningful subgroups with opposing renal responses were identified. Age, preoperative renal function, and the American Society of Anesthesiologists physical status classification emerged as dominant effect modifiers.

### Conclusions

This study illustrates how causal machine learning can reveal multidimensional treatment heterogeneity in perioperative datasets. This enables clinicians to anticipate individual responses and tailor vasopressor strategies accordingly. The mechanistic hypotheses presented promising avenues for targeted physiological research.

**How to cite this article**
Cui J, Lim E, Wu X, et al. (December 22, 2025) Phenylephrine's Heterogeneous Renal Effects in Non-Cardiac Surgery: A Causal Machine Learning Study. Cureus J Comput Sci 2 : es44389-025-00018-2. DOI https://doi.org/10.7759/s44389-025-00018-2

**Categories:** Health Informatics, Machine Learning (ML)
**Keywords:** phenylephrine, renal function, causal machine learning, heterogeneous effect, non-cardiac surgery

# Introduction

Intraoperative hypotension is common during surgery and a key factor significantly associated with an increased incidence of postoperative complications [1-3]. Maintaining the mean arterial pressure ⩾65 mmHg in non-cardiac surgeries is recommended to reduce the risk of postoperative complications [4,5]. Phenylephrine is one of the most commonly used vasopressor agents in surgical settings, acting through systemic vascular resistance [6,7].

In clinical practice, significant heterogeneity is often observed in the responses of patients undergoing intermediate-to-major non-cardiac surgery to phenylephrine [8]. Anesthesiologists must carefully balance these responses, as inappropriate use will increase the risk of renal hypoperfusion. Current guidelines [9-12] focus on individual risk factors rather than their combinations. As a result, managing multi-factorial patient conditions often depends heavily on practitioners' clinical experience and judgment.

Perioperative treatment is undergoing a profound transformation, moving away from standardised protocols toward precision interventions specifically tailored to individual variability [13,14]. This shift is facilitated by advancements in artificial intelligence and the integration of big data, aiming to achieve personalised, predictive, and real-time feedback-driven perioperative management [15-18]. Identifying and understanding the multidimensional heterogeneous responses to phenylephrine have become critical prerequisites for developing effective treatment strategies.

The kidneys are particularly vulnerable among various organ systems affected by intraoperative hemodynamic management. Renal function is highly sensitive to haemodynamic fluctuations during the perioperative period. According to KDIGO (Kidney Disease Outcomes Quality Initiative) guidelines [19], the glomerular filtration rate (GFR) is the standard index for evaluating renal function, stratified into five stages based on decreasing filtration capacity. GFR measured during the acute postoperative phase can effectively reflect the physiological impact of phenylephrine on renal perfusion pressure and filtration function. Prior studies [8,20,21] have indicated that the selective α-1 agonistic effect of phenylephrine may adversely affect postoperative renal function through mechanisms such as altering renal cortical blood flow distribution and increasing renal vascular resistance.

Despite the growing number of related studies, there remains a lack of an analytical framework capable of elucidating the causal relationship between intraoperative phenylephrine use and acute postoperative renal function. This study aimed to address this gap. In recent years, integrating causal inference with machine learning has provided a novel approach for modelling individualised treatment effects in multidimensional clinical data [22,23]. By integrating several state-of-the-art machine learning models, this study aimed to explore the multidimensional heterogeneous effects of phenylephrine on postoperative acute renal function in patients undergoing intermediate-to-major non-cardiac surgery from the perspective of causal machine learning.

# Materials And Methods

## Study population and data source

This study used fully de-identified, publicly available, and high-resolution perioperative data from the VitalDB database [24], which was originally approved for public release by the Institutional Review Board of Seoul National University Hospital. This database comprises 6,388 surgical cases collected between 2016 and 2019, with each case encompassing detailed intraoperative monitoring, drug administration records, laboratory test results, and postoperative outcomes. Data preprocessing followed a structured workflow: raw VitalDB files were extracted in comma-separated format, synchronised by case identifiers, and time-series variables were aggregated to summary statistics (mean, minimum, maximum, and last pre-extubation values). Variables with missingness >10 % were excluded; the remaining were imputed using multiple imputation by chained equations (MICE) to preserve variance and avoid listwise deletion.

For this study, the key variables that were selected were based on the monitoring and safety guidelines recommended by the Anesthesia Patient Safety Foundation. The core features included invasive arterial pressure, heart rate, end-tidal carbon dioxide, the American Society of Anesthesiologists (ASA) Physical Status Classification System, intraoperative phenylephrine usage, and renal biomarkers. Variables with a missing rate exceeding 10% were excluded to ensure data quality. Missing values in the remaining variables were imputed using MICE. This approach constructed conditional regression models for each variable with missing values, utilised the remaining variables as predictors, and iteratively estimated and filled in the missing data. Complete data before and after imputation are presented in Figure *1*.

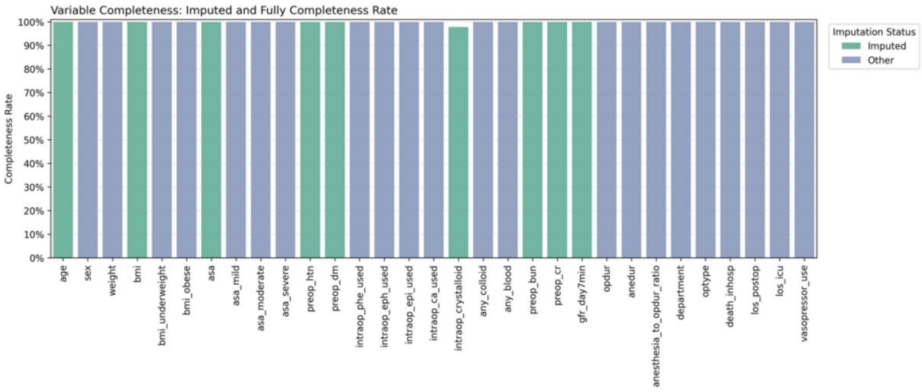


**FIGURE 1: Variable-level data completeness and imputation status in the analytical dataset**

X-axis: Variable names (e.g., preoperative creatinine, BUN, BMI, ASA, etc.)

Y-axis: Percentage of completeness (% of non-missing data)

ASA, American Society of Anesthesiologists physical status classification system; BMI, Body Mass Index; BUN, Blood Urea Nitrogen

## Selection of outcomes and treatment variables

For this study, the acute postoperative phase is referred to the first 7 days following surgery. This phase was characterised by heightened physiological stress, marked instability in key homeostatic indicators, and an increased risk of postoperative complications [25]. According to the KDIGO guidelines [19], renal function is categorised into five stages based on GFR. As detailed in Table *1*, each stage reflects a progressive degree of kidney function impairment and declining filtration efficiency. The KDIGO guidelines [19] further specify that the evaluation of postoperative acute kidney failure (AKI) involves detecting continuous variations in renal function.

| Stage | GFR (ml/min/1.73 m²) | Functional Status | Clinical Interpretation |
|---|---|---|---|
| G1 | ≥ 90 | Normal or high | Normal kidney function; other signs of damage may be present |
| G2 | 60–89 | Mildly decreased | Slight decline in function |
| G3a | 45–59 | Mild to moderate decrease | Early signs of dysfunction may appear |
| G3b | 30–44 | Moderate to severe decrease | Increased risk of complications; requires close monitoring |
| G4 | 15–29 | Severe decrease | Significant functional impairment; often pre-dialysis stage |
| G5 | < 15 | Kidney failure | Dialysis or transplantation is usually required |

**TABLE 1: Classification of renal function stages based on estimated glomerular filtration rate (GFR), functional status, and clinical interpretation**

Among these metrics, the lowest postoperative GFR is a critical extreme value, acting as a dynamic target for clinical intervention. During surgery and in the immediate postoperative period, the kidneys often experience brief but significant fluctuations in perfusion pressure or ischemia-reperfusion injury [26]. Monitoring this lowest GFR value provides a sensitive indicator of transient haemodynamic fluctuations during the acute postoperative phase, aiding in the assessment of renal perfusion pressure and glomerular filtration function under physiological stress. For this study, the lowest GFR value within 7 days post-surgery was selected as the outcome variable. Standardised KDIGO AKI staging could not be applied due to limited availability of serial creatinine trajectories and urine output data in the dataset; therefore, lowest postoperative GFR was selected as a continuous and sensitive marker of acute renal physiological stress.

Additionally, the merits of defining phenylephrine exposure as a binary treatment variable (use and non-

use) or a continuous dosage measure were carefully evaluated. The binary formulation ensures compatibility with widely validated causal inference frameworks, such as doubly robust estimators, and ensemble-based treatment effect learners. While this binary exposure definition enables stable causal estimation within established causal machine learning frameworks, it does not capture dose, timing, or duration effects, which may contribute additional clinically relevant heterogeneity.

## Covariate selection

Based on the backdoor criterion [27] and widely accepted covariate adjustment practices in causal machine learning [28,29], covariates to effectively control potential confounding factors and enhance the internal validity of the study's estimation were systematically classified. A hybrid selection strategy was employed to combine the propensity score models with clinical expertise to evaluate causal relevance. The propensity score results are presented in Figure *2*. Confounding factors were defined as preoperative or intraoperative variables that could simultaneously influence phenylephrine usage and postoperative renal function. Outcome-only variables were defined as pre-treatment variables affecting postoperative renal function outcomes but unrelated to the decision to use vasopressor drugs.

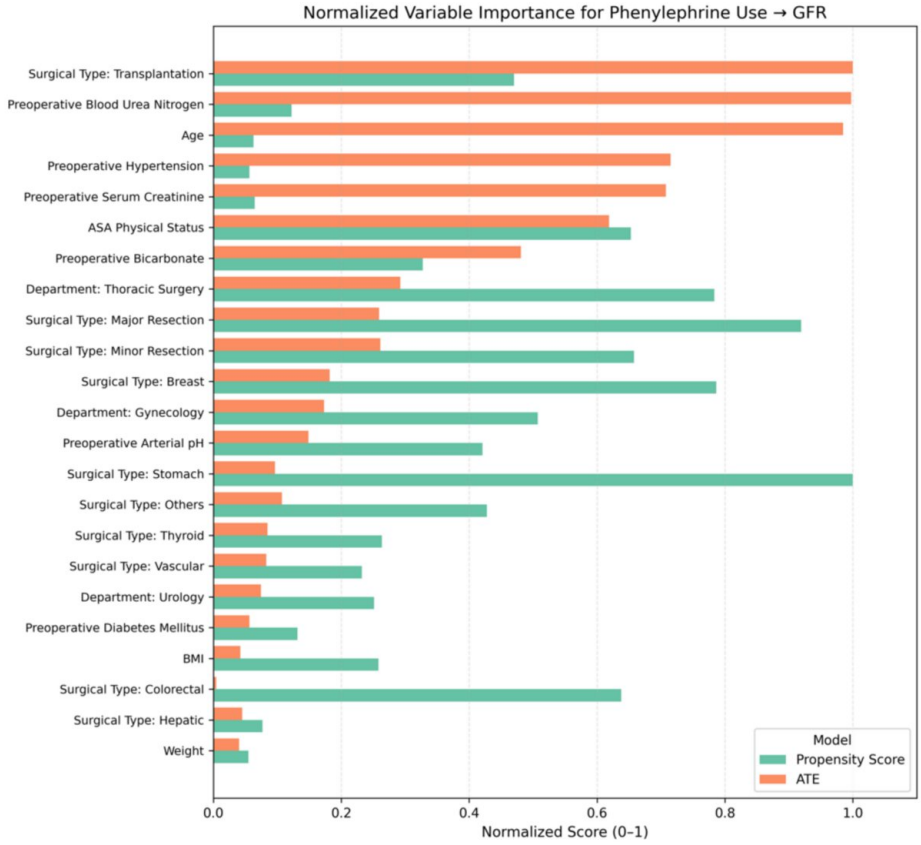


**FIGURE 2: Normalised variable importance for estimating the effect of intraoperative phenylephrine use on postoperative GFR in the PS and ATE models**

X-axis: Normalised score (0–1)

Y-axis: Covariate names (e.g., age, BMI, hypertension, ASA, preoperative creatinine, BUN, etc.)

ASA, American Society of Anesthesiologists physical status classification system; ATE, Average Treatment Effect; BMI, Body Mass Index; BUN, Blood Urea Nitrogen; GFR, Glomerular Filtration Rate; PS, Propensity Score

## Statistical analysis and model development

This dataset was divided into a training set (70%) and a validation set (30%), stratified according to the proportion of the treatment exposure group to ensure balanced representation of the exposed and unexposed groups in both subsets. Descriptive statistics were used to summarise patient characteristics across the total, training, and validation datasets. Key variables in the descriptive analysis included patient demographics (age, gender, and body mass index [BMI]), preoperative clinical parameters (serum

creatinine, blood urea nitrogen, serum bicarbonate, and arterial blood pH value), drug exposure during surgery (phenylephrine, ephedrine, epinephrine, and calcium administration), and surgical category. Continuous variables were expressed as mean ± standard deviation and compared using the independent samples t-test. Categorical variables were reported as counts and percentages, with group differences assessed using the Chi-square test. All p-values were calculated to assess baseline comparability between the training and validation sets. Model implementation was performed in Python 3.10 using Scikit-learn v1.5 and XGBoost v2.0. Hyperparameter tuning for each algorithm employed five-fold cross-validation with grid search to minimise out-of-sample bias. Model selection was guided by two criteria: (1) post-inverse probability of treatment weighting (IPTW) covariate balance (mean standardised mean difference [SMD] < 0.1) and (2) smooth overlap of propensity score distributions between treated and control groups. Feature scaling and categorical encoding (one-hot for binary, ordinal for ordered variables) were applied before model training.

## Causal inference assumptions

This analysis relies on standard causal inference assumptions: unconfoundedness (no unmeasured confounders given observed covariates), positivity (sufficient overlap in covariate distributions), and SUTVA (no interference between units). While these assumptions cannot be definitively tested, we assess their plausibility through covariate balance evaluation and propensity score overlap analysis. Despite extensive covariate adjustment and the use of doubly robust estimators, this study remains observational in nature and cannot fully exclude residual confounding. Intraoperative factors such as the depth and duration of hypotension, fluid responsiveness, anesthetic depth, and cardiac output were not explicitly modelled and may influence both vasopressor use and postoperative renal outcomes.

## Propensity score model selection

To identify an optimal propensity score model for IPTW, nine popular candidate models were systematically evaluated: logistic regression, random forest, XGBoost, multilayer perceptron, gradient boosting, support vector machine, CatBoost, LightGBM, and naïve Bayes. Hyperparameter tuning for each model was performed using grid search with cross-validation on the training dataset.

Evaluation was based on two pre-specified criteria: covariate balance was assessed by calculating the mean SMD across all covariates after IPTW; and the distributional characteristics of the propensity scores were examined, focusing on the degree of overlap between the treatment and control groups, to ensure a smooth, unimodal shape that satisfies the positivity assumption. The optimal model parameters obtained are used to calculate the stabilised IPTW weights for downstream causal effect estimation.

## Individual and heterogeneous treatment effect estimation

Multiple complementary causal inference approaches were employed to estimate individual-level treatment effects (ITE) of intraoperative phenylephrine administration on postoperative renal function. The primary estimator in this study was the augmented inverse probability weighting (AIPW) method, a doubly robust approach that integrates outcome modelling with inverse probability of treatment weighting. The model was configured with a total of 100 decision trees. Additionally, two ensemble-based meta-learning frameworks were employed: the T-Learner and the X-Learner. All models were trained using the same set of baseline covariates. Each causal learner estimated the conditional average treatment effect for every individual record using the identical covariate set defined in the propensity model. AIPW was implemented as a doubly-robust estimator combining outcome regression and inverse weighting. The T- and X-Learners employed gradient-boosted decision trees with 100 estimators and learning rate 0.05. Estimation performance was evaluated by comparing average treatment effect (ATE) stability across bootstrapped resamples (n = 1,000) to ensure consistency of effect direction and magnitude.

The distribution of ITE on postoperative GFR using violin plots was visualised. Subgroup definitions were based on previous studies [8] that identified these factors as potential modifiers of treatment effect heterogeneity. Stratified analyses were conducted across combined subgroups of sex, BMI, hypertension, and ASA classification. Patients were stratified according to BMI (classified into four equal parts following the WHO standards), presence of hypertension, ASA classification (divided into ASA 1, ASA 2, and ASA ⩾ 3), and age (categorised into 18-44 years, 45-65 years, and ⩾65 years). From the perspective of statistical independence, ASA classification indicates overall physical condition, whereas age captures age-related functional variations. Both variables exhibit relatively low collinearity in the modelling process. In contrast, BMI and hypertension exhibit clinical correlation, with BMI being a known risk factor for hypertension. To avoid over-controlling similar mechanisms, a 2×3 subgroup framework was constructed.

## Causal distillation and SHAP-based interpretation framework

A causal distillation tree (CDT) was constructed to approximate the ITE derived from a causal forest model. The CDT, fitted using a shallow decision tree, acts as a sparse surrogate model that optimally partitions the data into interpretable subgroups. The model was configured with a maximum tree depth limited to three levels. A random forest regressor on the IPTW-weighted validation set was trained for

prediction-level attribution, and SHapley Additive exPlanations (SHAP) values were calculated using TreeExplainer.

To enhance interpretability and avoid reliance on black-box models [30,31], input features based on existing studies [8,32,33] were grouped into six clinically coherent domains. Specifically, the preoperative renal function domain included preoperative creatinine and blood urea nitrogen. The demographics domain encompassed patient age. The comorbidities domain covered preoperative hypertension and diabetes. The ASA status domain included binary indicators for ASA physical status levels 1 through 4. The surgical type domain incorporated procedure-related variables such as transplantation, major resection, and thoracic surgery. The intraoperative drugs domain comprised intraoperative administration of ephedrine, calcium, and epinephrine. The grouped SHAP bar chart illustrates the importance of each variable group in the model's predictions. The Beeswarm chart visualises the individualised influence directions and distributions of variable groups across different patients. The random seed was set to 42 to ensure reproducibility of the results. All the analyses and calculations were conducted using Google Colab version 1.2.0. Model interpretability was achieved by extracting SHAP values from the IPTW-weighted random forest regressor and averaging them across all trees to obtain mean absolute SHAP importance. For the CDT, pruning was applied when node sample size <5% of total to prevent overfitting. The resulting tree provides an interpretable approximation of the underlying causal forest structure, highlighting key variable thresholds driving treatment heterogeneity.

# Results And Discussion

## Results

*Experimental Setup*

All analyses were conducted in Google Colab (v1.2.0) using Python 3.10 and established scientific libraries (NumPy, Pandas, Scikit-learn, and SHAP). The analytical workflow consisted of three stages: (1) propensity score estimation and covariate balancing through IPTW using the optimised XGBoost model; (2) individual treatment effect estimation using AIPW, T-Learner, and X-Learner frameworks; and (3) interpretability analysis combining a CDT and SHAP. The dataset was randomly divided into training (70%) and validation (30%) subsets, and all random seeds were fixed at 42 to ensure reproducibility. Model performance and stability were assessed by comparing consistency of ATE estimates across learners and confirming post-IPTW covariate balance (all SMD < 0.1).

*Patient Characteristics and Baseline Data*

This study included 3,017 adult patients undergoing intermediate-to-major non-cardiac surgery, with 2,111 allocated to the training set and 906 to the validation set. The proportion of the treatment-exposed group was 24.4% in both sets. Figure *3* illustrates the inclusion and exclusion criteria. Table *2* summarises the baseline demographic, physiological, and surgical characteristics of the cohort.

No statistically significant differences were observed in any baseline covariates between the training and validation sets (all P values > 0.05). The average age of the patients was 60.4 ± 13.6 years, and the average BMI was 23.0 ± 3.6 kg/m$^2$, consistent with the characteristics of a general adult surgical population. The median ASA physical status classification was 2 (mean 1.92 ± 0.64), indicating that most patients had mild to moderate systemic diseases.

Preoperative laboratory tests indicated generally normal renal function (i.e., estimated GFR > 60 mL/min/1.73m$^2$), with an average serum creatinine level of 0.82 ± 0.35 mg/dL and an estimated GFR of 86.7 ± 25.3 mL/min/1.73 m$^2$. Acid-base parameters, including preoperative arterial pH (7.36 ± 0.08) and bicarbonate (24.0 ± 3.9 mmol/L), were within the physiological range, and preoperative haemodynamics were stable overall. A total of 12 variables were retained as confounding factors, while 10 were designated as outcome-only variables.

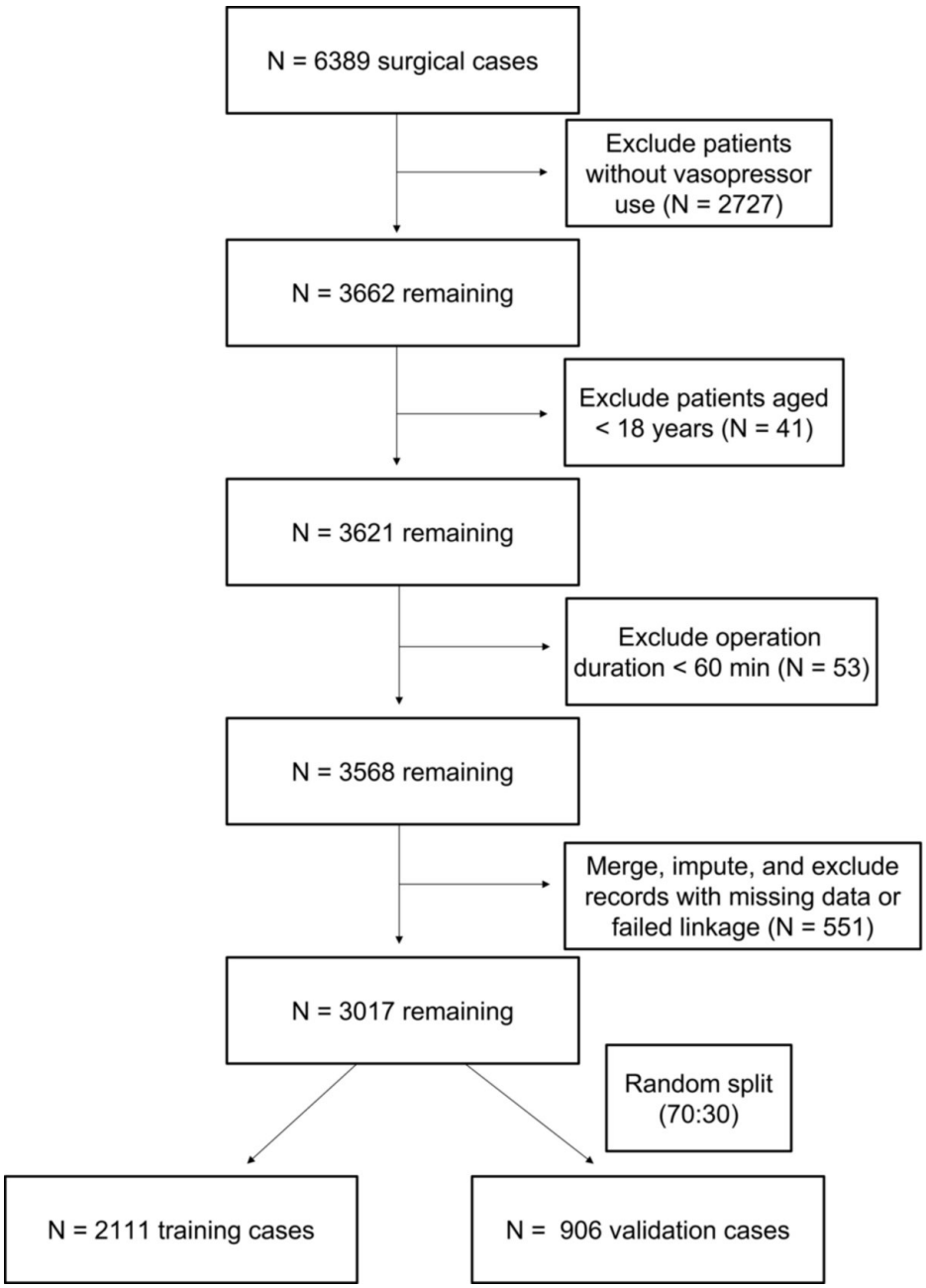


**FIGURE 3: Study cohort selection and data preprocessing workflow**

| Variable | Total (n = 3,017) | Training (n = 2,111) | Validation (n = 906) | p-value |
|---|---|---|---|---|
| age | 60.43 ± 13.56 | 60.70 ± 13.44 | 59.80 ± 13.84 | 0.0946 |
| bmi | 23.02 ± 3.59 | 23.05 ± 3.62 | 22.96 ± 3.52 | 0.5247 |
| asa | 1.92 ± 0.64 | 1.93 ± 0.64 | 1.90 ± 0.66 | 0.3361 |
| preop_ph | 7.36 ± 0.08 | 7.36 ± 0.08 | 7.36 ± 0.08 | 0.9716 |
| preop_hco3 | 23.97 ± 3.94 | 24.03 ± 4.05 | 23.84 ± 3.67 | 0.2997 |
| preop_bun | 10.36 ± 6.36 | 10.35 ± 6.38 | 10.37 ± 6.30 | 0.9441 |
| preop_cr | 0.76 ± 0.80 | 0.75 ± 0.68 | 0.79 ± 1.03 | 0.2424 |
| height | 162.36 ± 8.51 | 162.34 ± 8.55 | 162.39 ± 8.41 | 0.8866 |
| weight | 60.83 ± 11.36 | 60.89 ± 11.48 | 60.69 ± 11.09 | 0.654 |

| | | | | |
|---|---|---|---|---|
| intraop_crystalloid | 1523.97 ± 1523.85 | 1497.88 ± 1501.04 | 1584.76 ± 1574.91 | 0.1558 |
| anesthesia_to_opdur_ratio | 1.31 ± 0.16 | 1.31 ± 0.16 | 1.31 ± 0.17 | 0.9031 |
| opdur | 185.82 ± 103.58 | 184.63 ± 103.41 | 188.60 ± 103.99 | 0.3346 |
| anedur | 232.42 ± 111.30 | 231.11 ± 111.31 | 235.48 ± 111.26 | 0.3231 |
| preop_htn = 0.0 (No HTN) | 1929 (63.9%) | 1349 (63.9%) | 580 (64.0%) | 0.4885 |
| preop_htn = 1.0 (Yes HTN) | 1088 (36.1%) | 762 (36.1%) | 326 (36.0%) | |
| preop_dm = 0.0 (No DM) | 2659 (88.1%) | 1869 (88.5%) | 790 (87.2%) | 0.5893 |
| preop_dm = 1.0 (Yes DM) | 358 (11.9%) | 242 (11.5%) | 116 (12.8%) | |
| intraop_phe_binary = 0 | 2280 (75.6%) | 1595 (75.6%) | 685 (75.6%) | 0.358 |
| intraop_phe_binary = 1 | 737 (24.4%) | 516 (24.4%) | 221 (24.4%) | |
| intraop_eph_used = 0 | 339 (11.2%) | 240 (11.4%) | 99 (10.9%) | 0.3908 |
| intraop_eph_used = 1 | 2678 (88.8%) | 1871 (88.6%) | 807 (89.1%) | |
| intraop_phe_used = 0 | 2280 (75.6%) | 1595 (75.6%) | 685 (75.6%) | 0.358 |
| intraop_phe_used = 1 | 737 (24.4%) | 516 (24.4%) | 221 (24.4%) | |
| intraop_epi_used = 0 | 2935 (97.3%) | 2058 (97.5%) | 877 (96.8%) | 0.7294 |
| intraop_epi_used = 1 | 82 (2.7%) | 53 (2.5%) | 29 (3.2%) | |
| intraop_ca_used = 0 | 2202 (73.0%) | 1562 (74.0%) | 640 (70.6%) | 0.4953 |
| intraop_ca_used = 1 | 815 (27.0%) | 549 (26.0%) | 266 (29.4%) | |
| any_colloid = 0 | 2587 (85.7%) | 1823 (86.4%) | 764 (84.3%) | 0.7515 |
| any_colloid = 1 | 430 (14.3%) | 288 (13.6%) | 142 (15.7%) | |
| any_blood = 0 | 2695 (89.3%) | 1889 (89.5%) | 806 (89.0%) | 0.3515 |
| any_blood = 1 | 322 (10.7%) | 222 (10.5%) | 100 (11.0%) | |
| asa_mild = 0 | 468 (15.5%) | 329 (15.6%) | 139 (15.3%) | 0.8136 |
| asa_mild = 1 | 2549 (84.5%) | 1782 (84.4%) | 767 (84.7%) | |
| asa_moderate = 0 | 2639 (87.5%) | 1842 (87.3%) | 797 (88.0%) | 0.2566 |
| asa_moderate = 1 | 378 (12.5%) | 269 (12.7%) | 109 (12.0%) | |
| asa_severe = 0 | 2985 (98.9%) | 2089 (99.0%) | 896 (98.9%) | 1 |
| asa_severe = 1 | 32 (1.1%) | 22 (1.0%) | 10 (1.1%) | |
| bmi_underweight = 0 | 2745 (91.0%) | 1922 (91.0%) | 823 (90.8%) | 0.1575 |
| bmi_underweight = 1 | 272 (9.0%) | 189 (9.0%) | 83 (9.2%) | |
| bmi_obese = 0 | 2916 (96.7%) | 2038 (96.5%) | 878 (96.9%) | 0.6467 |
| bmi_obese = 1 | 101 (3.3%) | 73 (3.5%) | 28 (3.1%) | |
| asa_high = 0 (ASA < 3) | 2606 (86.4%) | 1819 (86.2%) | 787 (86.9%) | 0.4206 |
| asa_high = 1 (ASA ≥ 3) | 411 (13.6%) | 292 (13.8%) | 119 (13.1%) | |
| department = General surgery | 2450 (81.2%) | 1696 (80.3%) | 754 (83.2%) | 0.8592 |
| department = Gynecology | 105 (3.5%) | 73 (3.5%) | 32 (3.5%) | |
| department = Thoracic surgery | 402 (13.3%) | 299 (14.2%) | 103 (11.4%) | |
| department = Urology | 60 (2.0%) | 43 (2.0%) | 17 (1.9%) | |
| optype = Biliary/Pancreas | 288 (9.5%) | 186 (8.8%) | 102 (11.3%) | 0.9421 |
| optype = Breast | 133 (4.4%) | 95 (4.5%) | 38 (4.2%) | |

| | | | |
|---|---|---|---|
| optype = Colorectal | 566 (18.8%) | 388 (18.4%) | 178 (19.6%) |
| optype = Hepatic | 186 (6.2%) | 125 (5.9%) | 61 (6.7%) |
| optype = Major resection | 285 (9.4%) | 200 (9.5%) | 85 (9.4%) |
| optype = Minor resection | 178 (5.9%) | 129 (6.1%) | 49 (5.4%) |
| optype = Others | 345 (11.4%) | 258 (12.2%) | 87 (9.6%) |
| optype = Stomach | 486 (16.1%) | 344 (16.3%) | 142 (15.7%) |
| optype = Thyroid | 123 (4.1%) | 87 (4.1%) | 36 (4.0%) |
| optype = Transplantation | 278 (9.2%) | 186 (8.8%) | 92 (10.2%) |
| optype = Vascular | 149 (4.9%) | 113 (5.4%) | 36 (4.0%) |

**TABLE 2: Baseline demographic, physiological, and preoperative laboratory characteristics of the cohort, stratified by training and validation datasets**

ASA, American Society of Anesthesiologists physical status classification system; DM, Diabetes Mellitus; HTN, Hypertension

*Selection and Evaluation of the Propensity Score Model*

Table *3* summarises the optimal hyperparameter configurations and the corresponding mean SMD after IPTW for each evaluated model. After hyperparameter tuning via cross-validated grid search, each model was trained on the training set with its optimal configuration and subsequently evaluated on the testing set. Figure *4* displays the propensity score distributions generated by nine models.

| Model | Best Params |
|---|---|
| Random Forest | {'n_estimators': 400, 'max_depth': 40, 'min_samples_split': 5, 'min_samples_leaf': 10, 'max_features': 'sqrt', 'bootstrap': True} |
| LightGBM | {'num_leaves': 31, 'max_depth': 1, 'learning_rate': 0.05, 'n_estimators': 300, 'min_child_samples': 10, 'subsample': 0.8, 'colsample_bytree': 0.8, 'reg_alpha': 0, 'reg_lambda': 0.1} |
| XGBoost | {'n_estimators': 400, 'max_depth': 8, 'learning_rate': 0.01, 'subsample': 0.8, 'colsample_bytree': 0.8, 'gamma': 0, 'reg_lambda': 1, 'reg_alpha': 0, 'scale_pos_weight': 3.0910852713178296} |
| GradientBoosting | {'n_estimators': 300, 'learning_rate': 0.01, 'max_depth': 5, 'min_samples_split': 2, 'min_samples_leaf': 1, 'subsample': 0.8, 'max_features': 'sqrt'} |
| LogisticRegression | {'penalty': 'l2', 'C': 0.1, 'solver': 'lbfgs', 'max_iter': 1000, 'class_weight': 'balanced'} |
| SVM | {'C': 10, 'gamma': 0.1, 'kernel': 'rbf'} |
| MLP | {'hidden_layer_sizes': (64,), 'activation': 'tanh', 'solver': 'lbfgs', 'alpha': 0.001, 'learning_rate_init': 0.01, 'max_iter': 1000} |
| NaiveBayes | {'var_smoothing': 1e-07} |
| CatBoost | {'iterations': 300, 'depth': 6, 'learning_rate': 0.01, 'l2_leaf_reg': 3, 'subsample': 0.8, 'colsample_bylevel': 0.8} |

**TABLE 3: Optimal parameters of nine models**

CatBoost, Category Boosting; LightGBM, Light Gradient Boosting Machine; MLP, Multi-Layer Perceptron; SVM, Support Vector Machine; XGBoost, eXtreme Gradient Boosting

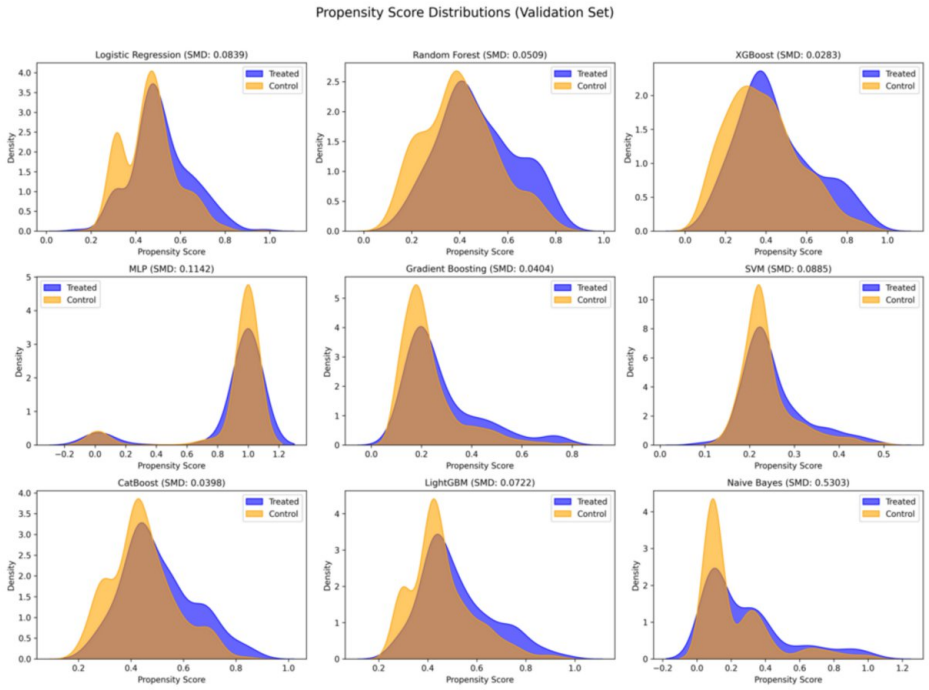


**FIGURE 4: Comparison of propensity score distributions estimated by nine machine learning models**

CatBoost, Category Boosting; LightGBM, Light Gradient Boosting Machine; MLP, Multi-Layer Perceptron; SMD, Standardised Mean Difference; SVM, Support Vector Machine; XGBoost, eXtreme Gradient Boosting

Ultimately, XGBoost was selected as the final propensity score model for implementing IPTW. This decision was based on XGBoost achieving the best covariate balance, with a post-IPTW mean SMD of 0.0283. XGBoost exhibited the most favourable propensity score distribution, characterised by smooth, unimodal density curves and a substantial region of common support between the treated and control groups. Figure *5* shows that IPTW successfully reduced the SMD of all included covariates below the threshold of 0.1.

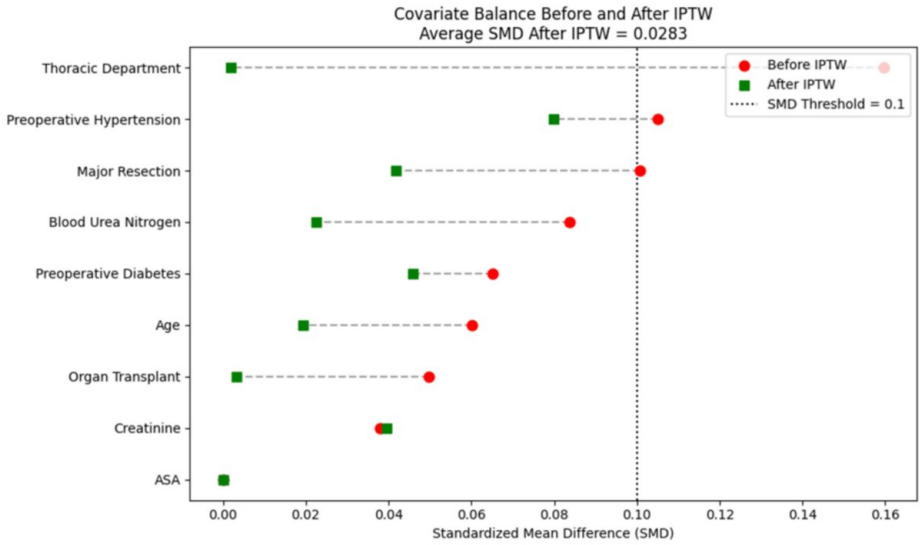


**FIGURE 5: Covariate balance before and after IPTW, assessed by SMD**

X-axis: Covariate names

Y-axis: Standardised Mean Difference (SMD)

IPTW, Inverse Probability of Treatment Weighting

*Stratified Renal Effect Analysis*

Figure *6* displays the estimated distribution of postoperative ITE on GFR using the AIPW estimator. The distribution resembles a normal shape but is centred around a negative mean (ATE = -3.24), suggesting a slight overall decrease in postoperative GFR following intraoperative phenylephrine administration, while significant heterogeneity exists in patients' responses.

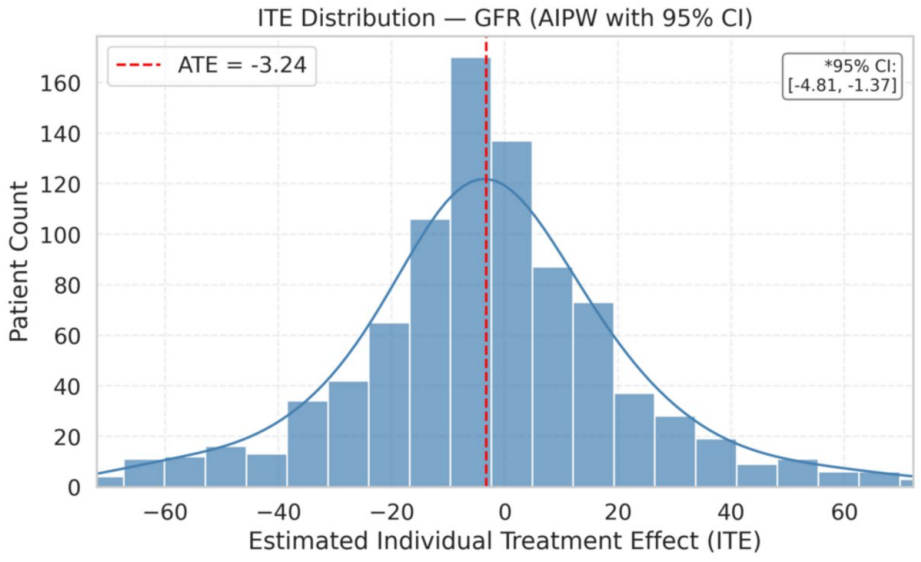


**FIGURE 6: Distribution of ITE on postoperative GFR estimated by AIPW**

AIPW, Augmented Inverse Probability Weighting; ATE, Average Treatment Effect; GFR, Glomerular Filtration Rate; ITE, Individual-level Treatment Effects

Figures *7*-*8* illustrate the ITE distributions estimated using T-Learner and X-Learner based on gradient boosting decision trees. The estimated ATE by the T-Learner was -0.71 (95% CI: -0.96 to -0.37), while the X-Learner yielded a slightly larger effect of -0.55 (95% CI: -1.16 to -0.2). Both distributions consistently

indicate heterogeneity in patients' responses to intraoperative phenylephrine. Figure 9 presents a detailed stratified analysis of ITE on postoperative GFR. Figure 9A shows the greatest postoperative GFR decline in 45-65-year-olds with normal BMI and ASA 3+. Figure 9B shows the greatest postoperative GFR improvement in patients aged 65 and older with hypertension and ASA 3+. Patients with similar clinical characteristics demonstrated opposing directions of estimated treatment effects. These findings demonstrate substantial variability in individual treatment effects across clinically defined subgroups. Some subgroup strata were relatively small; subgroup-specific estimates should therefore be interpreted as hypothesis-generating.

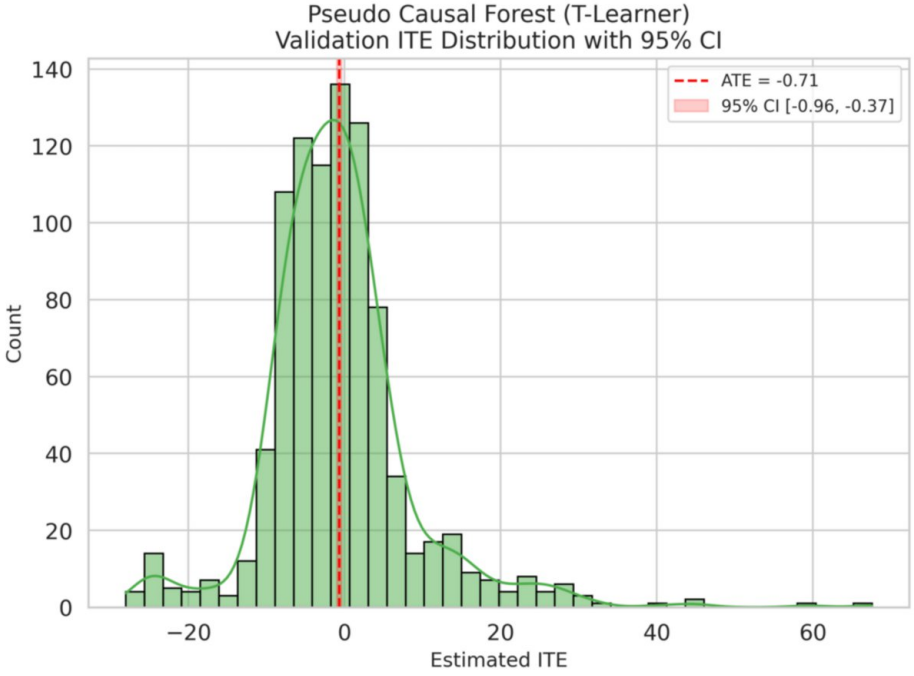


**FIGURE 7: Estimated ITE distributions and ATE with 95% confidence intervals from T-Learner model**

ATE, Average Treatment Effect; ITE, Individual-level Treatment Effects

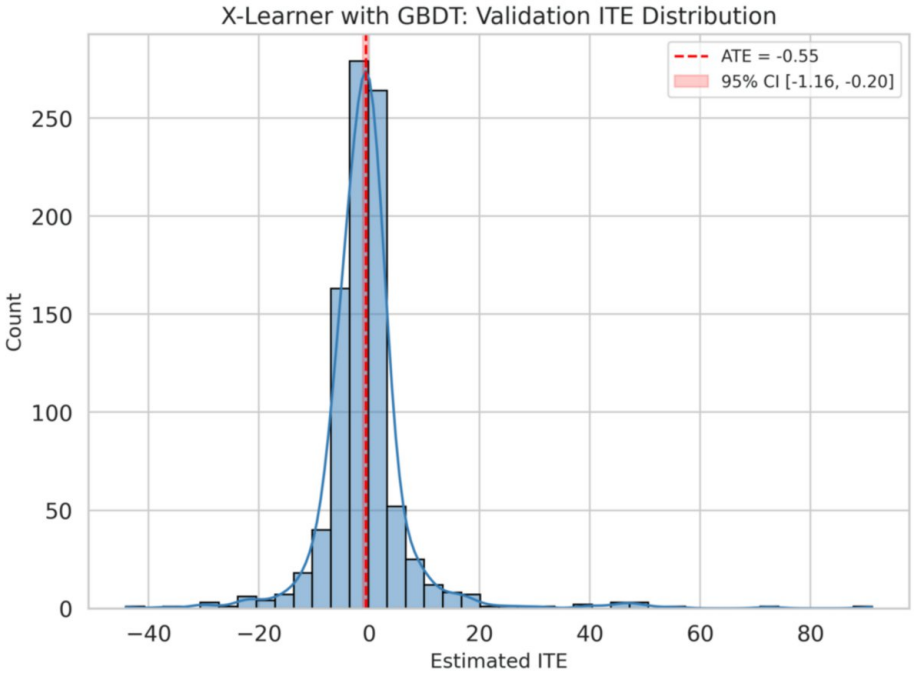


**FIGURE 8: Estimated ITE distributions and ATE with 95% confidence intervals from X-Learner model**

ATE, Average Treatment Effect; GBDT, Gradient Boosted Decision Trees; ITE, Individual-level Treatment Effects

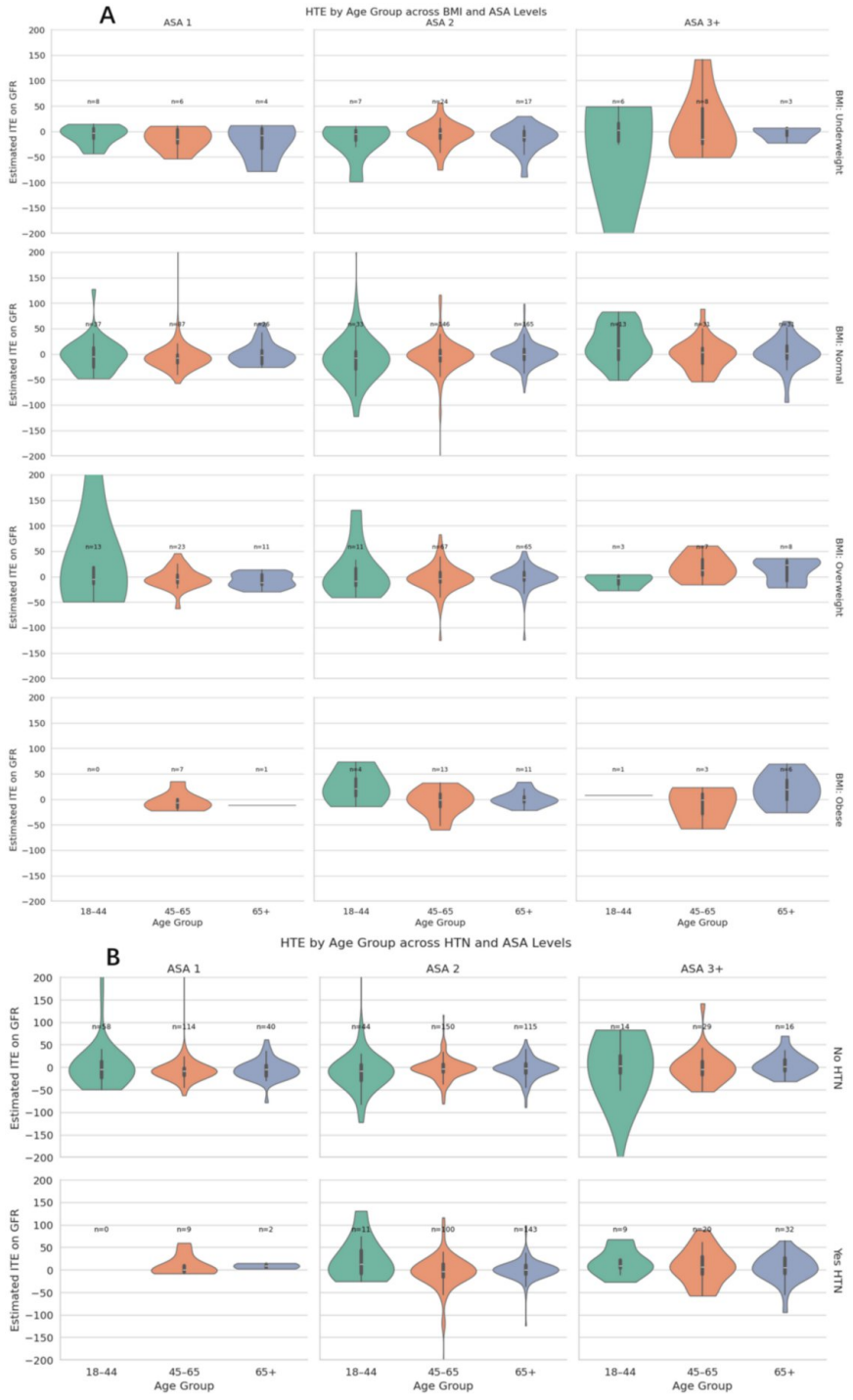


**FIGURE 9: Heterogeneous effects of phenylephrine on postoperative GFR across patient subgroups**

ASA, American Society of Anesthesiologists physical status classification system; BMI, Body Mass Index; GFR, Glomerular Filtration Rate; HTE, Heterogeneous Treatment Effects; HTN, Hypertension; ITE, Individual-level Treatment Effects

*Model Interpretability*

Figure *10* displays a CDT (with all values expressed in standardised units). The most negatively impacted subgroup (preop_bun ⩽ -0.038, age ⩽ 0.485, ASA ⩽ 1.221) exhibited an average ITE of -8.003 mL/min/1.73 $m^2$, corresponding to -8.21 mL/min/1.73 $m^2$ after back-transformation. In contrast, elderly patients with preoperative hypertension (preop_htn > 0.292) and preserved renal function (preop_cr ⩽ 0.239) showed positive treatment effects, with an average ITE of 2.521 mL/min/1.73 $m^2$. This subgroup had an average

ITE of 5.43 mL/min/1.73 m², representing the most favorable estimated renal benefit. Other subgroups with positive effects included patients with lower preoperative serum creatinine levels (preop_cr ⩽ -0.043), suggesting postoperative improvement of renal function.

Figure *11A* shows the aggregated SHAP importance scores by clinical characteristic categories. Preoperative renal function variables are the most influential predictors of postoperative GFR, followed by demographic characteristics, ASA status, and comorbidities. Figure *11B* presents the distribution and directional contribution of SHAP values across various clinical domains. Lower preoperative renal function is consistently associated with negative SHAP values, indicating a downward impact on the prediction of postoperative GFR. The ASA status exhibits a moderate but consistent pattern, where higher ASA scores are associated with negative SHAP values, leading to a prediction of decreased postoperative GFR. CDT and SHAP analyses consistently identified age and preoperative renal function as dominant contributors to heterogeneity in postoperative GFR response.

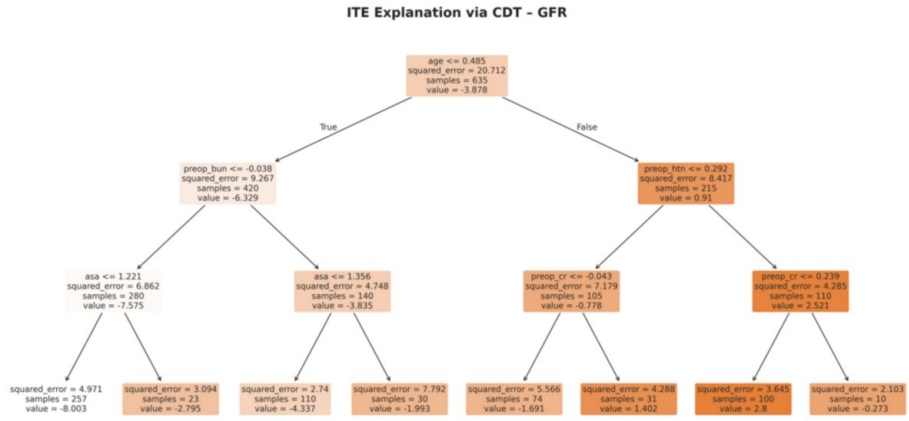


**FIGURE 10: CDT analysis of ITE on GFR following intraoperative phenylephrine use**

CDT, Causal Distillation Tree; GFR, Glomerular Filtration Rate; ITE, Individual-level Treatment Effects

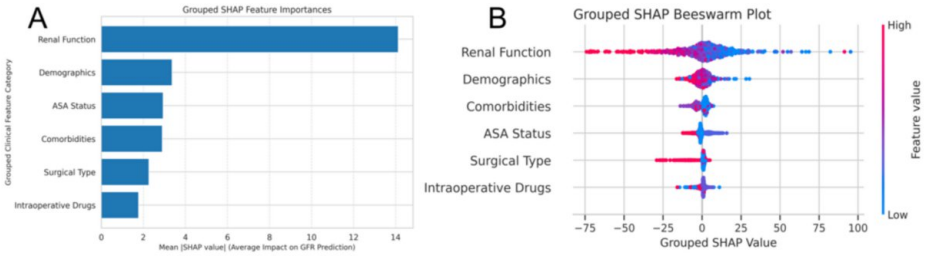


**FIGURE 11: Grouped SHAP summary and beeswarm plots**

ASA, American Society of Anesthesiologists physical status classification system; GFR, Glomerular Filtration Rate; SHAP, SHapley Additive exPlanation

## Discussion

*Key Findings and Clinical Implications*

Phenylephrine is a commonly used vasopressor drug in surgical settings. This study's findings indicate that using phenylephrine during intermediate to major non-cardiac surgeries exhibits multi-dimensional heterogeneity in its impact on postoperative acute kidney function. It elucidates this heterogeneity and aims to provide novel insights for perioperative precision medication strategies in non-cardiac surgeries. The SHAP plots quantify the marginal contributions of different variables to model predictions, offering complementary insights to the CDT analysis. Clinically, these findings suggest that phenylephrine should not be considered uniformly renal-protective or harmful. Patient-specific characteristics, particularly age, baseline renal reserve, and overall physiological status, should inform vasopressor selection and titration during intermediate-to-major non-cardiac surgery.

*Interpretation of Critical Threshold Subgroups*

Figure *9* demonstrates that patients aged 18-44 with lower ASA scores, no hypertension, or normal/low BMI experience a decline in postoperative GFR. Conversely, patients over 65 with ASA 3+, hypertension, or high BMI show improved postoperative GFR.

The identification of critical threshold subgroups warrants further attention. Among patients aged 45-65 with normal or overweight weight, those with ASA grade 2 show an improvement in postoperative GFR, whereas those with ASA grade 3 or above exhibit the opposite trend. Among middle-aged overweight patients, subclinical components of metabolic syndrome, including microvascular remodelling, endothelial dysfunction, and early-stage renal arteriosclerosis, may elevate the lower limit of renal autoregulation. The vasoconstriction induced by phenylephrine might be excessive, increasing renal vascular resistance and reducing renal perfusion pressure, thereby inducing perfusion insufficiency.

In obese patients aged 45-65 years with ASA grade 2, postoperative GFR increases, while in elderly patients aged 65 years and above, postoperative GFR declines. From a haemodynamic perspective, middle-aged obese patients may exhibit subclinical metabolic syndrome, exacerbating the dysregulation of renal vascular tension and creating a paradox of volume excess but perfusion insufficiency [34]. It can be hypothesised that these patients may often maintain sufficient intravascular volume and relatively preserved vascular compliance, leading to α-adrenergic receptor-mediated vasoconstriction to elevate systemic blood pressure without significantly compromising glomerular perfusion, thereby sustaining or improving filtration rate.

In contrast, elderly patients are more prone to arterial stiffness, decreased pressure receptor sensitivity, and structural changes in renal microcirculation, leading to an elevated threshold of renal vascular autoregulation. The vasoconstriction induced by phenylephrine may excessively enhance renal vascular resistance, causing a drop in renal perfusion pressure. This assumption is consistent with findings reported in previous studies [8]. For such patients, starting with a low dose and gradually increasing it is recommended.

*Age-Related Variations in Treatment Response*

In 18-44-year-olds with ASA grade 2, patients without hypertension exhibit postoperative GFR improvement, while those with hypertension show no benefit or a slight decline. Young patients without hypertension have a lower autoregulation threshold, allowing α-receptor activation mediated by phenylephrine to moderately increase mean arterial pressure without significantly increasing renal vascular resistance, thereby improving renal perfusion and enhancing GFR.

However, young patients with hypertension exhibit long-term contraction adaptation in the renal arterioles, resulting in an upward shift in the autoregulation threshold, decreased endothelial reactivity, and increased sensitivity of renal vessels to α-agonists [8]. As a result, the enhanced vasoconstrictive effect of exogenous vasopressors may reduce renal blood flow and impair perfusion.

*Insights From CDT Analysis*

Figure *10* demonstrates that the root node of the CDT is stratified by age, indicating that baseline vascular physiological characteristics closely associated with age play a pivotal role in modulating renal responses. Postoperative GFR improved significantly in non-hypertensive patients aged ⩾45 with normal preoperative creatinine, indicating a low perfusion risk profile. Phenylephrine use effectively increases perfusion pressure and enhances filtration rate in this group. Notably, even a mild elevation in preoperative creatinine is associated with a rapid reversal of this therapeutic benefit. This reversal may be due to a breakdown in renal autoregulatory capacity. Under mild renal injury, renal arterioles exhibit reduced tolerance to changes in blood flow, and exogenous vasopressor drugs may induce the redistribution of blood flow, thereby reducing renal cortical perfusion and further impairing filtration function.

In patients aged 18-44 years with diminished renal function reserve, the presence or absence of hypertension constitutes a key determinant of phenylephrine treatment response direction. When renal function reserve is compromised, these individuals are more prone to insufficient renal blood flow perfusion and decreased filtration function postoperatively [35]. This study hypothesises that the renal vessels of hypertensive patients have adapted chronically to a high-perfusion environment, and the vasopressor effect of phenylephrine restores their habitual perfusion pressure, preventing filtration decline due to inadequate perfusion.

*SHAP Analysis and Variable Importance*

Figure *11A* illustrates that preoperative renal function characteristics dominate the prediction of GFR.

Multiple studies have also shown that preoperative GFR is an independent risk indicator for major postoperative complications [36-38]. A decrease in GFR rate is associated with an elevated risk of adverse outcomes.

Although the average contribution of remaining variable groups is lower, their SHAP distribution range is broader in Figure *11B*, indicating highly individualised impacts on prediction results. The predictive contributions of these variables exhibit significant nonlinearity and background dependence, which may be amplified under specific physiological conditions, triggering highly personalised model responses. Future research should focus on elucidating the nonlinear regulatory pathways of these variables and their interaction mechanisms with renal haemodynamics.

*Limitations and Future Directions*

This study has several important limitations that should be considered when interpreting the findings. First, the analysis is observational in nature and therefore cannot establish definitive causal relationships. Although extensive covariate adjustment and the use of doubly robust causal machine learning estimators were employed, residual confounding from unmeasured intraoperative factors, such as the depth and duration of hypotension, dynamic fluid responsiveness, anesthetic depth, and cardiac output, cannot be fully excluded.

Second, phenylephrine exposure was defined as a binary variable (use versus non-use). While this approach facilitates stable estimation within established causal inference frameworks, it does not capture potentially important clinical dimensions such as dose, timing, infusion rate, or duration of administration, which may contribute additional heterogeneity in renal responses.

Third, postoperative renal function was assessed using the lowest estimated GFR within 7 days after surgery. Standardised KDIGO AKI staging could not be applied due to the limited availability of serial creatinine trajectories and urine output data in the dataset. As a result, direct comparison with studies using categorical AKI definitions may be limited.

Fourth, some of the identified subgroups contained relatively small sample sizes. Subgroup-specific estimates should therefore be interpreted as hypothesis-generating rather than definitive evidence of differential treatment effects.

Fifth, this study was conducted using data from a single centre. Although this ensures consistency in data collection and clinical practice patterns, it may limit generalisability to other institutions with different perioperative protocols or patient populations. External validation in independent perioperative cohorts is required before clinical deployment of these findings.

Future research should focus on prospective validation of the identified heterogeneous treatment effects, incorporation of dose-response and timing-specific analyses of vasopressor use, and replication across multicentre datasets. Such efforts will be essential to determine the robustness, transportability, and clinical utility of personalised vasopressor strategies in non-cardiac surgery.

## Conclusions

This study illustrates how causal machine learning can reveal multidimensional treatment heterogeneity in perioperative datasets. It transforms the understanding of phenylephrine's effects and provides novel insights and a foundation for precision perioperative medicine, enabling clinicians to anticipate individual responses and tailor vasopressor strategies accordingly. The study findings suggest that the renal effects of phenylephrine vary significantly across multidimensional subgroups, with interacting factors such as age, BMI, ASA status, and renal function producing directionally opposite outcomes. This heterogeneity underscores the importance of personalised approaches to intraoperative haemodynamic management, particularly in patients with complex comorbidities or at high risk for postoperative renal dysfunction.

The clinical implications of the study findings extend beyond the specific context of phenylephrine use to broader considerations in perioperative medicine. This study contributes to the evolving paradigm of precision perioperative care by identifying patient subgroups with differential responses to vasopressor therapy. Future research should focus on prospectively validating these findings and developing clinical decision-support tools that incorporate patient-specific factors to guide individualised hemodynamic management strategies during surgery.

## Additional Information

### Author Contributions

All authors have reviewed the final version to be published and agreed to be accountable for all aspects of the work.

**Concept and design:** Chi Eung Danforn Lim, Enoch Chi Ngai Lim, Junqi Cui, Xiaoqin Wu

**Acquisition, analysis, or interpretation of data:** Chi Eung Danforn Lim, Enoch Chi Ngai Lim, Junqi Cui, Xiaoqin Wu

**Drafting of the manuscript:** Chi Eung Danforn Lim, Enoch Chi Ngai Lim, Junqi Cui, Xiaoqin Wu

**Critical review of the manuscript for important intellectual content:** Chi Eung Danforn Lim, Enoch Chi Ngai Lim, Junqi Cui, Xiaoqin Wu

**Supervision:** Chi Eung Danforn Lim

## Disclosures

**Human subjects:** All authors have confirmed that this study did not involve human participants or tissue. **Animal subjects:** All authors have confirmed that this study did not involve animal subjects or tissue. **Conflicts of interest:** In compliance with the ICMJE uniform disclosure form, all authors declare the following: **Payment/services info:** All authors have declared that no financial support was received from any organization for the submitted work. **Financial relationships:** All authors have declared that they have no financial relationships at present or within the previous three years with any organizations that might have an interest in the submitted work. **Other relationships:** All authors have declared that there are no other relationships or activities that could appear to have influenced the submitted work.

# References

1. Wijnberge M, Schenk J, Bulle E, et al.: Association of intraoperative hypotension with postoperative morbidity and mortality: systematic review and meta-analysis. BJS Open. 2021, 5:zraa018. 10.1093/bjsopen/zraa018
2. Qin G, Du MC, Yi KX, Gong Y: Intraoperative hypotension and postoperative risks in non-cardiac surgery: a meta-analysis. BMC Anesthesiology. 2025, 25:103. 10.1186/s12871-025-02976-5
3. Xiao C, Yang M, Cao L, Chen F, Jing S, Tan Y, Li H: The impact of intraoperative hypotension on postoperative acute kidney injury, mortality and length of stay following off-pump coronary artery bypass grafting surgery: a single-center retrospective cohort study. BMC Anesthesiology. 2024, 24:224. 10.1186/s12871-024-02616-4
4. Kristensen SD, Knuuti J, Saraste A, et al.: 2014 ESC/ESA Guidelines on non-cardiac surgery: cardiovascular assessment and management: The Joint Task Force on non-cardiac surgery: cardiovascular assessment and management of the European Society of Cardiology (ESC) and the European Society of Anaesthesiology (ESA). European Heart Journal. 2014, 35:2383-2431. 10.1093/eurheartj/ehu282
5. Halvorsen S, Mehilli J, Cassese S, et al.: 2022 ESC Guidelines on cardiovascular assessment and management of patients undergoing non-cardiac surgery: Developed by the task force for cardiovascular assessment and management of patients undergoing non-cardiac surgery of the European Society of Cardiology (ESC) Endorsed by the European Society of Anaesthesiology and Intensive Care (ESAIC). European Heart Journal. 2022, 43:3826-3924. 10.1093/eurheartj/ehac270
6. Kalmar AF, Allaert S, Pletinckx P, et al.: Phenylephrine increases cardiac output by raising cardiac preload in patients with anesthesia induced hypotension. Journal of Clinical Monitoring and Computing. 2018, 32:969-976. 10.1007/s10877-018-0126-3
7. Benevides ML, Andrade BWB, Zambardino HMD, Benevides MAM: A prospective single-center Brazilian study investigating the efficacy and safety of prophylactic phenylephrine infusion for the management of hypotension during cesarean section under spinal anesthesia. Cureus. 2023, 15:e42156. 10.7759/cureus.42156
8. Khanna AK, Saha AK, Segal S: Association of the exclusive use of intraoperative phenylephrine for treatment of hypotension with the risk of acute kidney injury after noncardiac surgery. Anaesthesia Critical Care & Pain Medicine. 2023, 42:101224. 10.1016/j.accpm.2023.101224
9. Phenylephrine Hydrochloride Injection, USP - Prescribing Information. U.S. Food and Drug Administration. (2014). Accessed: May 27, 2025: https://www.accessdata.fda.gov/drugsatfda_docs/label/2014/204300lbl.pdf.
10. Amneal Pharmaceuticals LLC. Phenylephrine Hydrochloride Injection, USP 10 mg/mL - Prescribing Information. (2020). Accessed: May 27, 2025: https://www.amneal.com/wp-content/uploads/2021/03/PHEWS-04-Phenylephrine-PI.pdf.
11. Phenylephrine. Australian Injectable Drugs Handbook. 9th edition. (2023). Accessed: May 27, 2025: https://adpha.au/publicassets/245c2e89-4042-ee11-912c-00505696223b/Phenylephrine-v9-1.pdf.
12. British Columbia Emergency Health Service. Phenylephrine - Drug Monograph. (2025). Accessed: 27 May, 2025: https://handbook.bcehs.ca/drug-monographs/phenylephrine/.
13. Nirvik P, Kertai MD: Future of perioperative precision medicine: integration of molecular science, dynamic health care informatics, and implementation of predictive pathways in real time. Anesthesia & Analgesia. 2022, 134:900-908. 10.1213/ane.0000000000005966
14. Harris EP, MacDonald DB, Boland L, Boet S, Lalu MM, McIsaac DI: Personalized perioperative medicine: a scoping review of personalized assessment and communication of risk before surgery. Canadian Journal of Anesthesia/Journal canadien d'anesthésie. 2019, 66:1026-1037. 10.1007/s12630-019-01432-6
15. Feng Z, Bhat RR, Yuan X, et al.: Intelligent perioperative system: towards real-time big data analytics in surgery risk assessment. arXiv. 2017, 10.48550/arXiv.1709.10192
16. Bignami E, Panizzi M, Bellini V: Artificial intelligence for personalized perioperative medicine. Cureus. 2024, 16:e53270. 10.7759/cureus.53270
17. Ganskaia I, Abaimov S: Before and after: machine learning for perioperative patient care. arXiv. 2022, 10.48550/arXiv.2201.08095
18. Saria S, Rajani AK, Gould J, Koller D, Penn AA: Integration of early physiological responses predicts later

illness severity in preterm infants. Science Translational Medicine. 2010, 2:48ra65. 10.1126/scitranslmed.3001304
19. Khwaja A: KDIGO clinical practice guidelines for acute kidney injury. Nephron Clinical Practice. 2012, 120:c179-c184. 10.1159/000339789
20. Thiele RH, Nemergut EC, Lynch C 3rd: The clinical implications of isolated alpha1 adrenergic stimulation. Anesthesia & Analgesia. 2011, 113:297-304. 10.1213/ane.0b013e3182120ca5
21. Sear JW: Kidney dysfunction in the postoperative period. British Journal of Anaesthesia. 2005, 95:20-32. 10.1093/bja/aei018
22. Feuerriegel S, Frauen D, Melnychuk V, et al.: Causal machine learning for predicting treatment outcomes. Nature Medicine. 2024, 30:958-968. 10.1038/s41591-024-02902-1
23. Sanchez P, Voisey JP, Xia T, Watson HI, O'Neil AQ, Tsaftaris SA: Causal machine learning for healthcare and precision medicine. Royal Society Open Science. 2022, 9:220638. 10.1098/rsos.220638
24. Lee HC, Park Y, Yoon SB, Yang SM, Park D, Jung CW: VitalDB, a high-fidelity multi-parameter vital signs database in surgical patients. Scientific Data. 2022, 9:279. 10.1038/s41597-022-01411-5
25. Small C, Laycock HJJ: Acute postoperative pain management. British Journal of Surgery. 2020, 107:e70-e80. 10.1002/bjs.11477
26. Scholz H, Boivin FJ, Schmidt-Ott KM, Bachmann S, Eckardt KU, Scholl UI, Persson PB: Kidney physiology and susceptibility to acute kidney injury: implications for renoprotection. Nature Reviews Nephrology. 2021, 17:335-349. 10.1038/s41581-021-00394-7
27. Pearl J: Causality: Models, Reasoning, and Inference. Cambridge University Press, Cambridge; 2009. 10.1017/S0266466603004109
28. Mehrabi N, Morstatter F, Saxena N, Lerman K, Galstyan A: A survey on bias and fairness in machine learning. ACM Computing Surveys. 2021, 54:1-35. 10.1145/3457607
29. Brookhart MA, Schneeweiss S, Rothman KJ, Glynn RJ, Avorn J, Stürmer T: Variable selection for propensity score models. American Journal of Epidemiology. 2006, 163:1149-1156. 10.1093/aje/kwj149
30. Lundberg SM, Nair B, Vavilala MS, et al.: Explainable machine-learning predictions for the prevention of hypoxaemia during surgery. Nature Biomedical Engineering. 2018, 2:749-760. 10.1038/s41551-018-0304-0
31. Christodoulou E, Ma J, Collins GS, Steyerberg EW, Verbakel JY, Van Calster B: A systematic review shows no performance benefit of machine learning over logistic regression for clinical prediction models. Journal of Clinical Epidemiology. 2019, 110:12-22. 10.1016/j.jclinepi.2019.02.004
32. Malugari AR, Kumar KM, Silambanan S: Role of blood urea nitrogen to creatinine ratio in the assessment of hypovolemia who have undergone major surgeries - a cross-sectional study. The Egyptian Journal of Internal Medicine. 2024, 36:97. 10.1186/s43162-024-00363-z
33. Kim B, Sangha G, Singh A, Bohringer C: The effect of intraoperative hypotension on postoperative renal function. Current Anesthesiology Reports. 2023, 13:181-186. 10.1007/s40140-023-00564-2
34. Jang KW, Hur J, Lee DW, Kim SR: Metabolic syndrome, kidney-related adiposity, and kidney microcirculation: unraveling the damage. Biomedicines. 2024, 12:2706. 10.3390/biomedicines12122706
35. Sharma A, Mucino MJ, Ronco C: Renal functional reserve and renal recovery after acute kidney injury. Nephron Clinical Practice. 2014, 127:94-100. 10.1159/000363721
36. Mases A, Sabaté S, Dalmau A, et al.: Methadone is a local anaesthetic-like inhibitor of neuronal Na+ channels and blocks excitability of mouse peripheral nerves. British Journal of Anaesthesia. 2015, 114:110-120. 10.1093/bja/aeu206
37. Mooney JF, Ranasinghe I, Chow CK, et al.: Preoperative estimates of glomerular filtration rate as predictors of outcome after surgery: a systematic review and meta-analysis. Anesthesiology. 2013, 118:809-824. 10.1097/aln.0b013e318287b72c
38. Tanaka Y, Kanda M, Tanaka C, et al.: Usefulness of preoperative estimated glomerular filtration rate to predict complications after curative gastrectomy in patients with clinical T2-4 gastric cancer. Gastric Cancer. 2017, 20:736-743. 10.1007/s10120-016-0657-6